A High-Voltage Class D Audio Amplifier for Dielectric Elastomer Transducers

Nielsen, Dennis; Knott, Arnold; Andersen, Michael A. E.

Published in:
Proceedings of the 2014 IEEE Applied Power Electronics Conference and Exposition

Link to article, DOI:
10.1109/APEC.2014.6803776

Publication date:
2014

Document Version
Early version, also known as pre-print

A High-Voltage Class D Audio Amplifier for Dielectric Elastomer Transducers

Dennis Nielsen, Arnold Knott and Michael A. E. Andersen
Technical University of Denmark
Department of Electrical Engineering
Ørsteds plads 349, 2800 Kgs Lyngby
Email: deni@elektro.dtu.dk

***Abstract*— Dielectric Elastomer (DE) transducers have emerged as a very interesting alternative to the traditional electrodynamic transducer. Lightweight, small size and high maneuverability are some of the key features of the DE transducer. An amplifier for the DE transducer suitable for audio applications is proposed and analyzed. The amplifier addresses the issue of a high impedance load, ensuring a linear response over the midrange region of the audio bandwidth (100 Hz – 3.5 kHz). THD+N below 0.1% are reported for the $\pm$ 300 V prototype amplifier producing a maximum of 125 Var at a peak efficiency of 95 %.**

INTRODUCTION

Class D audio amplifiers are commonly used in sound reproduction driving electrodynamic transducers [1], [2], [3], [4], [5], [6], [7]. While these audio systems are dominating the market of sound reproduction, they suffer from the poor efficiency imposed by the electrodynamic transducer, and the weight of the electromagnet. As a consequence the audio community is constantly searching for new audio transducers. An alternative to the electrodynamic transducer is the electrostatic transducer. Electrostatic transducers are known from their usage in electrostatic loudspeakers, however Dielectric Elastomers (DE) can also be used to form an electrostatic transducer [8], [9], [10]. Such capacitive transducers present a high impedance, frequency depended nonlinear load to the amplifier. A DE transducer is shown in figure 1. The DE transducer is constructed by printing compliant electrodes on a thin piece of silicone. Commercial electrostatic loudspeakers are driven from tube, linear or audio-transformer based amplifier solutions. Consequently these systems suffer from being bulky, fragile and inefficient. In order to establish the full potential of the DE transducer, a new generation of audio amplifiers must be developed. These amplifiers should have a high power density, low power loss and be robust. Accordingly it is proposed to use a switch-mode audio amplifier or class D amplifier for driving the DE transducer [11], [12]. Class D audio amplifiers are known for their low power consumption, high power density and excellent audio figures (for instance low Total Harmonic Distortion plus Noise or THD+N) [4], [13], [1], [2]. In this paper a half-bridge based class D amplifier is proposed as amplifier for the DE transducer. A hysteretic based self-oscillating bandpass current mode control scheme is suggested, ensuring high loop gain and thus excellent THD+N. It should be noted, that DE transducers and their amplifiers are not limited to the application of sound reproduction. Micro-robotics with DE transducers is another application, which has recieved interest in recent years [14].

Fig. 1: DE actuator.

THEORY

When driving a DE transducer it is appropriate to give a formal definition of the term efficiency. The first order approximation will yield a capacitive load. Accordingly no real power will be delivered to the load. Efficiency will thus be defined as

$$\eta = \frac{P_{Out}}{P_{Out}+P_{In}} \tag{1}$$

where $P_{Out} = \frac{V_{rms}^2}{\left(\frac{1}{2\pi f_{Ref} C_{Deap}}\right)}$, the reactive power delivered to the load, and P_{In} corresponding to the real power consumed by the amplifier. This definition of the term efficiency will be used throughout the paper.

Losses

The paper analysis the power stage of figure 2. Notice, that the inductor current equals the current of C_{DE} ($i_L(t) = i_{C_{DE}}(t)$), because the parallel resistance of C_{DE}, R_P, has a value of 1 MΩ or above [10]. The current $i_L(t)$ is a superposition of the ripple ($\Delta i_L(D)$) and the sinusoidal reference or audio current ($i_{Ref}(t)$)

$$i_L(t) = \Delta i_L(D) + i_{Ref}(t) \tag{2}$$

The following definitions will be used

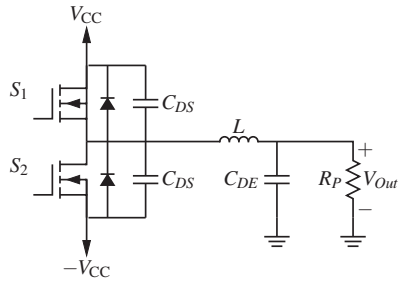

Fig. 2: Half-Bridge class D amplifier.

$$\Delta i_L(D) = \frac{1-D}{L} V_{CC} D T_{Sw} \tag{3}$$

The Root Mean Square (RMS) and Average (AV) value of 3 can be expressed as functions of the modulation index, M [15]. Using the relation $D(t) = \frac{1}{2}(Msin(2\pi f_{Ref} t) + 1)$ is can be shown that [15]

$$\Delta i_{L,RMS}(M) = \frac{V_{CC}}{4 L f_{Sw}} \sqrt{\frac{1-M^2}{3} + \frac{M^4}{8}} \tag{4}$$

The RMS value of the reference current is defined as

$$i_{Ref,RMS}(M) = \frac{V_{CC} M}{\sqrt{2}} 2\pi f_{Ref} C_{DE} \tag{5}$$

DE loss

The DE transducers is model as a capacitor with a series resistance, neglecting dielectric losses. Accordingly

$$P_{DE} = R_S i^2_{L,rms} \tag{6}$$

Magnetic loss

The magnetic loss is divided into conduction and ferrite loss. Conduction losses are defined as

$$P_{Cu} = R_{Cu} i^2_{L,rms} \tag{7}$$

with

$$R_{Cu} = \frac{\rho N l_T}{A_{Wire}} \tag{8}$$

N is the number of turns, l_T the average length of a turn, A_{Wire} the wire cross-sectional area and ρ the resistivity. Only single layer winding schemes are considered.

Steinmetz equation are used to estimate the ferrite loss

$$P_{Fe} = V_{Core} k_{Fe} \left(\left(\frac{f_{Ref}}{f_0} \right)^{\alpha} \left(\frac{B(i_{Ref})}{B_0} \right)^{\beta} + \left(\frac{f_{Sw}}{f_0} \right)^{\alpha} \left(\frac{B(\Delta i_L(M))}{B_0} \right)^{\beta} \right) \tag{9}$$

Greater accuracy can be achieved by use of the improved Steinmetz equation. However, for the purpose of this paper Equation (9) is sufficient.

Semiconductor loss

The semiconductor losses are divided into conduction and switching losses. The conductions loss caused by the MOSFET on resistance, $R_{DS_{On}}$, is

$$P_{DS_{On}} = R_{DS_{On}} i^2_{L,rms} \tag{10}$$

The switching loss can be approximated by [16]

$$P_{Sw} = \begin{cases} 4 f_{Sw} C_{DS} V^2_{CC} & i_{Ref}(M) \le \Delta i_L(M) \\ f_{Sw} V_{CC} \tau(i_{Ref}) \frac{\hat{I}_L}{\pi} + 4 f_{Sw} C_{DS} V^2_{CC} & i_{Ref}(M) > \Delta i_L(M) \end{cases} \tag{11}$$

with

$$\tau(I_L) = R_G Q_{GD} \left(\frac{1}{v_{GS,th} + \frac{I_L}{g}} + \frac{1}{V_G - v_{GS,th} - \frac{I_L}{g}} \right) \tag{12}$$

$$+ R_G C_{ISS} \ln \left(\frac{v_{GS,th} + \frac{I_L}{g}}{v_{GS,th}} \frac{V_G - v_{GS,th}}{V_G - v_{GS,th} - \frac{I_L}{g}} \right) \tag{13}$$

Zero voltage switching

Switching losses can be limited by ensuring soft switching or zero voltage switching (ZVS) of the MOSFETs. The quasi-square wave ZVS buck converter is analyzed in [17], and ZVS is guaranteed at 50 % duty cycle, if the switches are operated with sufficient deadtime. The deadtime can be evaluated as

$$t_{Dead} = \frac{\pi}{2} \sqrt{L C_{Sw}}. \tag{14}$$

The resonance tank of L and C_{Sw} reaches its maximum amplitude at $\frac{T}{4}$. T being the resonance period. C_{Sw} equals to two times the mosfet drain-source capacitance plus any other capacitive couplings at the switching node. The later includes coupling to the heatsink, the equivalent capacitance constructed from the output filter inductor parallel capacitance and C_{DEAP} etc.

Dead-time distortion

Several publications have analyzed the influence of pulse-timing errors on THD [18], [19], [16]. These are traditional divided into the categories of dead-time distortion, finite switching speed and conduction state errors. When operating the power stage at ZVS, the dead-time distortion becomes a key concern. It is shown in [16], that dead-time distortion is a function of the ratio between reference and ripple current. This section analyzes dead-time distortion for a class D amplifier driving a capacitive load. Voltage mode control is assumed, meaning that the output current no longer can be considered constant with respect to frequency. This is unlike the case of driving an electrodynamic loudspeaker, where the load typically is assumed being resistive, and those the output current does not change with frequency. Let the THD arising from dead-time distortion being defined as [16]

$$THD_d(M, \alpha_d, \alpha_I) = \frac{\Delta(\alpha_I) \sqrt{\sum_{i=2}^{N_{Max}} \left[2\alpha_d \frac{sin(i\frac{\pi}{2})}{i\frac{\pi}{2}} \right]^2}}{M - \alpha_d \frac{4}{\pi} \Delta(\alpha_I)}$$

where the dead-time delay factor is the ratio of the dead-time to the period of the switching frequency

$$\alpha_d = \frac{t_d}{T_{sw}} \tag{15}$$

and the ripple current factor

$$\alpha_I = \frac{\Delta i_L(M)}{i_{Ref}(M)} \tag{16}$$

The ripple current factor is the amplitude of the ripple current divided by the reference current. Both being functions of the modulation index, M.

Using the ripple current factor $\Delta(\alpha_I)$ of equation (15) is defined

$$\Delta(\alpha_I) = \begin{cases} 0 & i_{Ref}(M) \leq \Delta i_L(M) \\ \frac{\frac{\pi}{2} - arcsin(\alpha_I)}{\frac{\pi}{2}} & i_{Ref}(M) > \Delta i_L(M) \end{cases} \tag{17}$$

ANALYSIS

The following analysis assumes the basic design parameters of Table I. Using these parameters $\Delta i_L = 1.07A$. With a maximum output current of $300V2\pi3.5kHz100nF = 660mA$, the dead-time distortion does not compromise the overall THD even though the power stage is operated at ZVS.

TABLE I: Design parameters

	Designator	Value
Idle switching frequency	f_{Sw}	300 kHz
Output filter inductance	L	200 uH
DE Capacitance	C_{DE}	100 nF
Supply voltage	V_{CC}	$\pm$ 300 V
Closed-loop gain	A_V	43.5 dB
Loop time delay	t_D	250 ns
Hysteresis window	v_{Hyst}	720 mV
Bandwidth	f_{Ref}	100 Hz – 3.5 kHz

Parameters related to the losses are gathered in Table II. The output filter inductor is constructed using a T184-2 toroidal core from Micrometals, while the MOSFETs are of the type SPA08N80C3.

TABLE II: Parameters key to the loss analysis.

	Designator	Value
Drain-source on resistance	$R_{DS_{On}}$	650 mΩ
Drain-source capacitance	C_{DS}	16 pF
Number of inductor windings	N	92
DC resistance of output filter inductor	R_S	404mΩ

The individual loss components are plotted in figure 3 as function of the modulation index. Ferrite losses are the dominating ones.

IMPLEMENTATION

It is proposed to use a half-bridge power stage with hysteresis bandpass current mode control (BPCM), as amplifier for the DE transducer. BPCM control schemes for class D audio amplifiers driving electrodynamic transducers are well-known [6], [4], [20], [5], [21]. The big advantage of such control schemes is the fact, that stability is maintained, even when no resistive load is connected to the amplifier. As a consequence the zobel network used to damp the high Q of an unloaded amplifier can be eliminated [6]. Implementation of the BPCM scheme is achieved by either direct measurement or estimation of the inductor current [22], [8]. For this application the inductor current is measured using a current sense transformer. Accordingly an isolated feedback signal with enough bandwidth to handle the switching frequency is obtained. Figure 4(a) shows a schematic of the Class D amplifier with BPCM control scheme, while figure 4(b) gives the small-signal model of the amplifier.

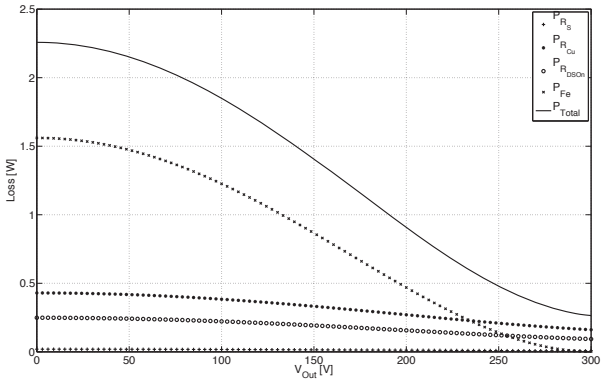

Fig. 3: Breakdown of losses.

A. Self-oscillation

Oscillation is ensured by shaping the open-loop frequency response to have a phase shift of 360 ^{o} and unity gain at the targeted switching frequency. This is the Barkhausen Oscillation criterium. It can be shown, that the switching frequency is described by the function [7], [6]

$$f_{Sw}(D) = \frac{D(1-D)}{2\frac{V_{Hyst}}{K} + t_D} \tag{18}$$

With K defined as:

$$K = 2V_{CC} \times step\{\lim_{s\to\infty} G_{Ctrl}(s)\} \tag{19}$$

For the purpose of designing the self-oscilation control loop, the controller transfer function must be defined

$$G_{Ctrl}(s) = \frac{v_{Carrier}(s)}{v_{PWM}(s)} \tag{20}$$

$$= G_{PI}(s)\left(K_{Vfb} + K_{Cfb}R_{Sense}N\frac{1+R_PC_{DEAPS}}{R_P}\right)\frac{1}{LC_{DEAP}s^2 + \frac{L}{R_P}s + 1} \tag{21}$$

K can be derived using equation (19) and (21)

$$K = \frac{2V_SK_{Cfb}NR_{Sense}}{L} \tag{22}$$

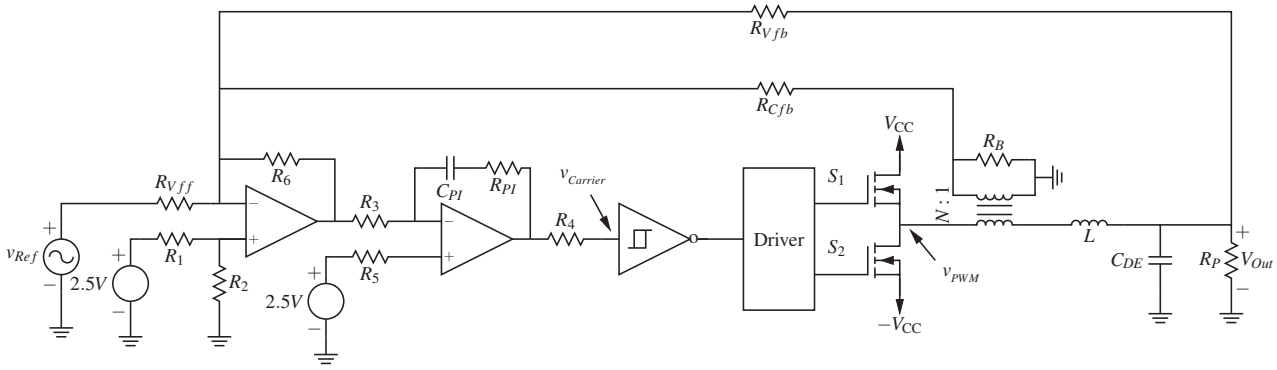

(a) Schematic with single-supply control circuitry.

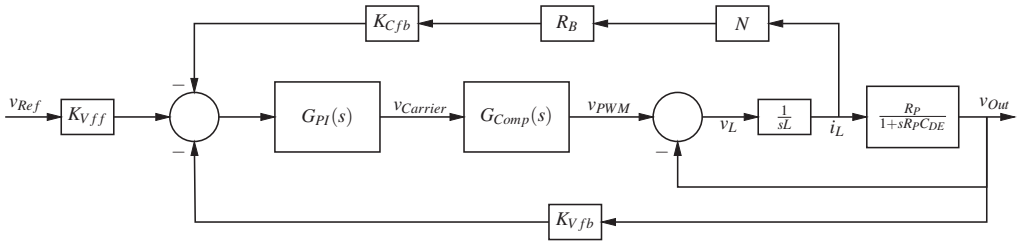

(b) Small-signal model.

Fig. 4: Half-brigde amplifier with BPCM control.

TABLE III: Component values

Component	Value
R_B	100 Ω
C_{PI}	10 nF
R_{PI}	1 $k\Omega$
R_{Cbf}	2 $k\Omega$
R_{Vff}	2 $k\Omega$
R_{Vfb}	300 $k\Omega$
R_1, R_2, R_3, R_4, R_5 and R_6	1 $k\Omega$
N	$\sqrt{\frac{200nH}{980uH}} \approx 0.014$

Experimental results

A prototype amplifier has been constructed. The amplifier operates from ± 300 V delivering a maximum power of 125 Var to a 100 nF capacitive load. Figure 5 shows the prototype amplifier, which is based on a Si8235 digital isolated gate driver. The BPCM control scheme are implemented using a single-supply control circuitry with a THS4221 comparator and LVM7219 operation amplifiers. Current measurement is preformed using the current sense transformer, CST1-070LB, of Coilcraft. A polypropylene capacitor is used as dummy load to perform all measurements. Table III shows the key component values of the prototype amplifier.

Efficiency

The measured efficiency is given in figure 6. The efficiency is defined in accordance with equation 1, and measured using the WT1600 digital power analyzer form Yokogawa. Note, that the efficiency at 100 Hz is below 42 %. Because the output voltage is kept fixed with respect to frequency, the reactive output power will drop inversely proportional with frequency. At 100 Hz the switching loss becomes comparable with the reactive output power. An efficiency above 90 % is achieved for the reference frequency 3.5 kHz. Voltage mode control of electrostatic transducers is preferred for applications were displacement is of concern. Charge mode control ensures greater linearity at the expense of displacement [23].

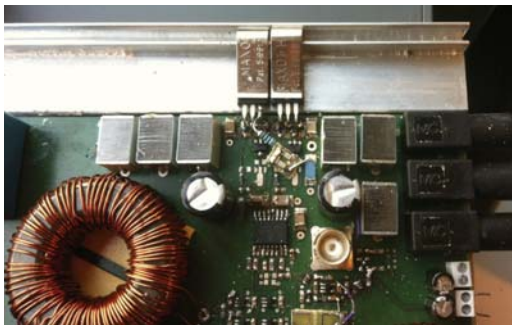

Fig. 5: Power stage used for the prototype amplifier.

THD+N and closed-loop response

THD+N is measured using an APX525 audio analyzer and a voltage attenuation interface. The voltage attenuation interface is necessary in order to protect the input-stage of the audio analyzer. Design and implementation of the voltage attenuation

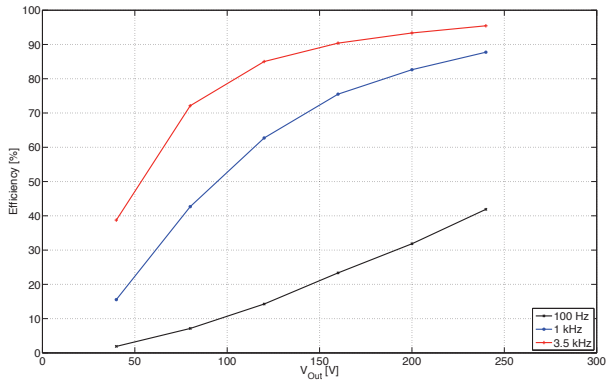

Fig. 6: Measured efficiency.

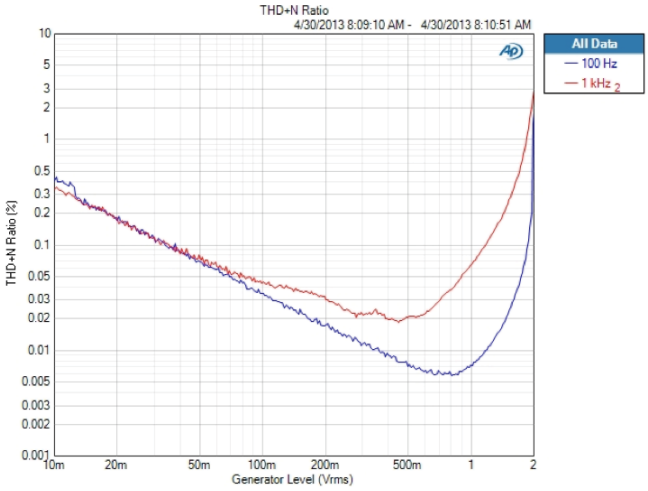

(a) THD+N for the reference frequencies of 100 Hz and 1 kHz.

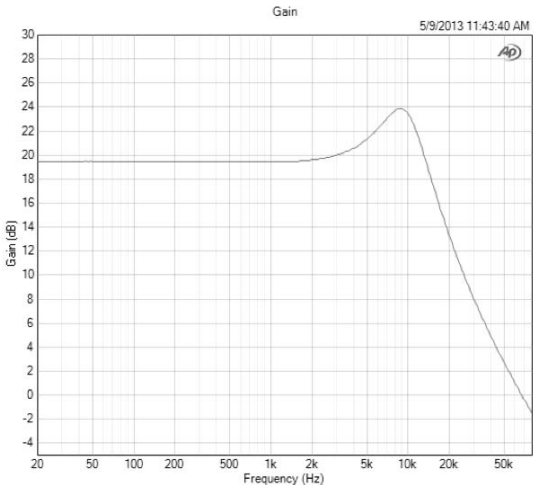

(b) Small-signal closed-loop response.

Fig. 7: Measuring results of prototype amplifier.

interface is well-described in the literature [11], [24]. Figure 7(a) gives the measured THD+N as function of the reference voltage for the frequencies of 100 Hz and 1 kHz. THD+N is below 0.1% over a significant part of the operation range. Noise is the dominating factor in the measured THD+N. The measured small-signal closed-loop frequency response is given in Figure 7(b). The response is flat (within 3 dB) over the midrange region of 100 Hz – 3.5 kHz.

Conclusion

A class D audio amplifier for dielectric elastomer transducers is proposed and analyzed. The amplifier addresses the issue of a high impedance load, ensuring a linear response over the midrange region of the audio bandwidth (100 Hz – 3.5 kHz), potentially paving the way for increased industry adoption of the highly promising technology of dielectric elastomers. THD+N below 0.1% are reported for the $\pm$ 300 V prototype amplifier producing a maximum of 125 Var at a peak efficiency of 94 %.

References

[1] S. Poulsen and M. A. E. Andersen, "Hysteresis controller with constant switching frequency," *Consumer Electronics, IEEE Transactions on*, vol. 51, no. 2, pp. 688–693, 2005.

[2] S. Poulsen and M. A. E. Andersen, "Simple pwm modulator topology with excellent dynamic behavior," in *Applied Power Electronics Conference and Exposition, 2004. APEC'04. Nineteenth Annual IEEE*, vol. 1. IEEE, 2004, pp. 486–492.

[3] S. Poulsen and M. A. Andersen, "Practical considerations for integrating switch mode audio amplifiers and loudspeakers for a higher power efficiency," in *Audio Engineering Society Convention 116*, 2004.

[4] S. Poulsen, "Towards active transducers," Ph.D. dissertation, Technical University of Denmark, July 2004.

[5] M. C. Høyerby and M. A. Andersen, "Derivation and analysis of a low-cost, high-performance analogue bpcm control scheme for class-d audio power amplifiers," in *Audio Engineering Society Conference: 27th International Conference: Efficient Audio Power Amplification*, 2005.

[6] M. C. W. Hoyerby and M. A. E. Andersen, "Carrier distortion in hysteretic self-oscillating class-d audio power amplifiers: Analysis and optimization," *IEEE Transactions On Power Electronics*, vol. 24, no. 3-4, pp. 714–729, Mar-Apr 2009.

[7] M. Høyerby and M. Andersen, "A small-signal model of the hysteretic comparator in linear-carrier self-oscillating switch-mode controllers," *Norpie*, 2006.

[8] R. Heydt, R. Kornbluh, R. Pelrine, and V. Mason, "Design and performance of an electrostrictive-polymer-film acoustic actuator," *Journal of Sound and Vibration*, vol. 215, no. 2, pp. 297–311, Aug. 1998.

[9] R. Heydt, R. Pelrine, J. Joseph, J. Eckerle, and R. Kornbluh, "Acoustical performance of an electrostrictive polymer film loudspeaker," *Journal of the Acoustical Society of America*, vol. 107, no. 2, pp. 833–839, Feb. 2000.

[10] R. Sarban, B. Lassen, and M. Willatzen, "Dynamic electromechanical modeling of dielectric elastomer actuators with metallic electrodes," *Mechatronics, IEEE/ASME Transactions on*, no. 99, pp. 1–8, 2011.

[11] D. Nielsen, A. Knott, and M. A. E. Andersen, "Driving capacitive transducers," in *Audio Engineering Society*, 134th Convention, Ed. Rome, Italy, 2013.

[12] D. Nielsen, A. Knott, and M. A. E. Andersen, "Hysteretic self-oscillating bandpass current mode control for class d audio amplifiers driving capacitive transducers," *ECCE ASIA*, 2013.

[13] K. Nielsen, "Audio power amplifier techniques with energy efficient power conversion," Ph.D. dissertation, Technical University of Denmark, 1998.

[14] C. Chen, Y. Tang, A. Khaligh, and R. W. Newcomb, "A low-power and high-gain converter for driving dielectric elastomer actuators," in *Applied Power Electronics Conference and Exposition (APEC), 2013 Twenty-Eighth Annual IEEE*, 2013, pp. 2755–2760.

[15] P. Ljusev and M. A. E. Andersen, "Single conversion stage amplifier - sicam," Ph.D. dissertation, Technical University of Denmark, 2006.
[16] K. Nielsen, "Linearity and efficiency performance of switching audio power amplifier output stages - a fundamental analysis," in *Audio Engineering Society Convention 105*, 9 1998.
[17] D. M. Robert W. Erickson, *Fundamental of power electronics*, 2nd ed. Springer, 2001, no. 978-0792372707.
[18] F. Koeslag, H. Mouton, and J. Beukes, "Analytical modeling of the effect of nonlinear switching transition curves on harmonic distortion in class d audio amplifiers," *Power Electronics, IEEE Transactions on*, vol. 28, no. 1, pp. 380–389, 2013.
[19] I. D. Mosely, P. Mellor, and C. Bingham, "Effect of dead time on harmonic distortion in class-d audio power amplifiers," *Electronics Letters*, vol. 35, no. 12, pp. 950–952, 1999.
[20] A. Rozman and J. Boylan, "Band pass current control," in *Applied Power Electronics Conference and Exposition, 1994. APEC'94. Conference Proceedings 1994., Ninth Annual*, 1994, pp. 631–637.
[21] P. Adduci, E. Botti, E. Dallago, and G. Venchi, "Pwm power audio amplifier with voltage/current mixed feedback for high-efficiency speakers," *Industrial Electronics, IEEE Transactions on*, vol. 54, no. 2, pp. 1141–1149, 2007.
[22] D. Qiu, S. Yip, H.-H. Chung, and S. Hui, "On the use of current sensors for the control of power converters," *Power Electronics, IEEE Transactions on*, vol. 18, no. 4, pp. 1047–1055, 2003.
[23] J. Borwick, *Loudspeaker and Headphone Handbook*, third edition ed. Reed Educational and Professional Publishing Ltd, 2001, no. 0 240 51578 1.
[24] A. P. Inc., "Measuring high impedance sources," *http://ap.com/kb/show/314*, 2010.